JOURNAL OF SOLID STATE CHEMISTRY 4, 80–86 (1972)

$La_xSr_{1-x}RuO_3$: A New Perovskite Series

R. J. BOUCHARD AND J. F. WEIHER

Central Research Department, E. I. du Pont de Nemours and Company, Experimental Station, Wilmington, Delaware 19898

Received: May 20, 1971

The compound $LaRuO_3$ was prepared for the first time. It appears to be metallic and antiferromagnetic. Solid solutions with ferromagnetic $SrRuO_3$ of the type $La_xSr_{1-x}RuO_3$ exist for all values of x. All compounds have the orthorhombic $GdFeO_3$-type perovskite structure. The ferromagnetism observed for $SrRuO_3$ ($x = 0$) diminishes rapidly with increasing La content, and antiferromagnetism or parasitic ferromagnetism sets in at approximately 35% La. All compounds show Curie–Weiss behavior at fairly low temperatures. The properties of $LaRhO_3$ are also discussed.

Introduction

The number of compounds with the perovskite structure having the general formula ABO_3 is legion. Typical oxidation states are $A^{+3}B^{+3}O_3$ and $A^{+2}B^{+4}O_3$, and the crystal structure is usually cubic or orthorhombic (D_{2h}^{16}-*Pbnm*, $Z = 4$), as typified by $GdFeO_3$. Magnetic and electrical transport properties can vary from metallic and Pauli paramagnetic, e.g., $LaNiO_3$ (*1*), through metallic and ferromagnetic, e.g., $SrRuO_3$ (*2*), to insulating and antiferromagnetic, e.g., $LaCrO_3$ (*1*). $SrRuO_3$ is particularly interesting since it represents the only known example where ferromagnetism results solely from a 2nd-row transition element. The metallic conductivity has been attributed (*2*, *3*) to a 2/3-filled, six-fold degenerate, π^*-type band formed by the interaction of the t_{2g} orbitals of Ru with suitably directed p orbitals of oxygen. We were interested in examining the effects on the magnetic and electrical properties of $SrRuO_3$ caused by substitution of the Sr^{+2} with a smaller trivalent cation like La^{+3}. This process would change the number of electrons in the π^*-band, adding one electron/La^{+3} as the formal valence of Ru changed from +4 in $SrRuO_3$ to +3 in $LaRuO_3$, simultaneously progressing from a 2/3 (d^4)- to a 5/6 (d^5)-filled band. In addition, we consider $LaRuO_3$ itself to be unusual, representing the only known example of Ru in a formally trivalent state in an oxide lattice.

Experimental

The starting materials for the $LaRuO_3$ end member were La_2O_3, RuO_2, and Ru metal, accurately weighed according to the reaction:

$$2La_2O_3 + 3RuO_2 + Ru \rightarrow 4LaRuO_3.$$

The La_2O_3 was high purity, heated to 1000°C ~ 16 hr, kept in a vacuum dessicator, and weighed quickly because of the well-known tendency of this oxide to react with atmospheric water and carbon dioxide. Preparation of "reactive" La_2O_3 by decomposition of the oxalate did not affect the reaction rate or the crystallinity of the product. The Ru metal was high-purity 325-mesh powder, which was also used to prepare the RuO_2 starting material by heating in O_2 at 1000°C for ~12 hr, grinding for 1 hr in a mechanical mortar grinder, and refiring at 1000°C in O_2 for another 12 hr. The resulting product had a single-phase rutile X-ray pattern and hydrogen reduction indicated RuO_2 stoichiometry within experimental error.

$SrRuO_3$ was prepared by firing $SrCO_3$ + Ru in O_2 at 1000°C, after Randall (*4*). The $SrRuO_3$ and the components of the $LaRuO_3$ (La_2O_3, RuO_2, and Ru) were mixed in the proper ratios to give $La_xSr_{1-x}RuO_3$ where $x = 0.1$, 0.25, 0.50, 0.75, and 1.

These starting materials were ground together for approximately 1 hr under dry nitrogen and quickly pressed into a pellet in a small hand press. The

pellet was then preheated to red heat in a silica tube under vacuum to remove any trace water picked up during the pressing operation and sealed in a Pt tube under vacuum. The tube was heated at 1300–1350°C for approximately 48 hr, then at 1100°C for approximately 48 hr, and cooled in the furnace. When silica tubes were used for the firing, or the 1100°C heating cycle was omitted, excess Ru was always present in the X-ray patterns.

A pellet of $LaRhO_3$ was also prepared. An equimolar mixture of La_2O_3 and Rh_2O_3 was ground for approximately 1 hr, pressed, sealed in Pt under vacuum, and fired at 1200°C for 16 hr. While the resultant product was reasonably well sintered and suitable for gross electrical characterization, X-ray examination revealed a trace of unreacted La_2O_3. Another sample was prepared by reaction at 1300°C and 3 kbar external pressure for 12 hr, slow cooled at 50°C/hr to 900°C, after which the furnace was shut off to cool. The product was now single-phase and noticeably more crystalline. This sample was used for obtaining X-ray data.

The products were examined with a Guinier–Hägg X-ray camera using an internal KCl standard ($a_0 = 6.2931$ Å) and monochromatic Cu$K\alpha$ radiation. The films were overexposed to emphasize the weak reflections. Cell dimensions were derived from a least-squares refinement of the *d*-values. For the ferromagnetic samples, a vibrating-sample magnetometer was used for magnetic susceptibility data, while a Faraday balance was used for the antiferromagnetic and diamagnetic compounds. Electrical resistivity was measured for two of the samples, using bars cut from polycrystalline pellets. Standard 4-probe techniques were employed. Attempts to grow single crystals by flux reactions for more accurate electrical data were unsuccessful.

Results and Discussion

A. Crystallographic

The products were single-phase, fairly well-crystallized orthorhombic perovskites. The space group *Pbnm* (same as $GdFeO_3$) was verified by the occurrence of the 021 reflection and the absence of the 201, which is not allowed. The refined lattice dimensions are listed in Table I. The parameters for $LaRuO_3$ are similar to those reported for $LaRhO_3$ (*5*) with a very slightly larger unit cell volume, reflecting the larger size of Ru^{+3} vs. Rh^{+3} (*6*). The refined lattice constants for $LaRhO_3$ are also included in Table I. They are in good agreement with Ref. (*5*). The *d*-values and relative intensities for $LaRuO_3$ are listed in Table II.

Volumes of the solid-solution unit cells vs. x in $La_xSr_{1-x}RuO_3$ will be the resultant of two opposing factors: (1) substitution of the smaller La^{+3} (1.18 Å) for Sr^{+2} (1.25 Å), and (2) substitution of the larger Ru^{+3} (0.68 Å) for Ru^{+4} (0.62 Å), using Shannon–Prewitt radii for the six-fold *B*-ion and eight-fold *A*-ion coordination in the orthorhombic perovskite (*6*). The observed cell volumes increase with increasing x, indicating factor 2 to be dominant. The lattice constants vs. x are plotted in Fig. 1. While the unit cell volume increases smoothly with x, the a, b, and c axes do not. The a and c axes appear to go through a maximum and there is a crossover from $a > b$ to $a < b$ at $x \sim 0.5$. Most striking is the rapid increase in b, the rate of increase becoming much larger at higher x. The large increase in the b-axis from $SrRuO_3$ to $LaRuO_3$ suggests that a factor other than size considerations may be important. Also, the dimensions for $SrRuO_3$ are much closer than $LaRuO_3$ to being cubic ($a = b = c/\sqrt{2}$ for cubic symmetry). This behavior may be related to the

TABLE I[a]

Compound	a(Å)	b(Å)	c(Å)	V(Å^3)
$LaRuO_3$	5.4944(6)	5.7789(5)	7.8548(7)	249.40(3)
$La_{.75}Sr_{.25}RuO_3$	5.5648(7)	5.6278(7)	7.8800(12)	246.78(4)
$La_{.5}Sr_{.5}RuO_3$	5.5777(2)	5.5749(8)	7.8881(5)	245.28(3)
$La_{.4}Sr_{.6}RuO_3$	5.5798(7)	5.5652(9)	7.8780(8)	244.63(4)
$La_{.25}Sr_{.75}RuO_3$	5.5782(7)	5.5488(6)	7.8646(12)	243.44(4)
$La_{.1}Sr_{.9}RuO_3$	5.5745(7)	5.5397(7)	7.8554(12)	242.58(5)
$SrRuO_3$	5.5702(4)	5.5324(4)	7.8494(7)	241.89(2)
$LaRhO_3$	5.5226(3)	5.7024(4)	7.9857(6)	248.65(2)

[a] Refined lattice dimensions for the $La_xSr_{1-x}RuO_3$ compounds and $LaRhO_3$. Numbers in parentheses are standard deviations in the last place.

TABLE II[a]

I/I_o	$h\,k\,l$	d_{obsd}	d_{calcd}
1	1 1 0	3.9812	3.9818
1	0 0 2	3.9256	3.9274
11	1 1 1	3.5498	3.5516
15	0 2 0	2.8882	2.8894
100	1 1 2	2.7970	2.7961
23	2 0 0	2.7477	2.7471
5	0 2 1	2.7114	2.7117
2	2 1 1 1 0 3	2.3654	2.3658
1	0 2 2	2.3273	2.3274
2	2 0 2	2.2521	2.2511
3	1 1 3	2.1879	2.1877
1	1 2 2	2.1423	2.1430
18	2 2 0	1.9910	1.9909
12	0 0 4	1.9639	1.9637
2	0 2 3	1.9401	1.9402
6	2 2 1	1.9300	1.9299
5	1 3 1	1.7711	1.7710
1	3 1 1	1.7042	1.7042
5	1 3 2	1.6498	1.6496
5	0 2 4	1.6241	1.6241
17	2 0 4 3 1 2	1.5968	1.5975
2	2 2 3	1.5854	1.5848
2	1 3 3	1.4932	1.4932
1	1 1 5 2 3 2	1.4620	1.4613
1	0 4 0	1.4447	1.4447
1	0 4 1	1.4208	1.4208
6	2 2 4 1 4 0	1.3981	1.3980
1	0 2 5	1.3795	1.3801
2	4 0 0	1.3733	1.3735
1	3 3 1 0 0 6	1.3087	1.3087

[a] X-Ray data for $LaRuO_3$. The intensities were estimated from relative peak heights on a diffractometer tracing. The observed d values were taken from a Guinier–Hägg film, and the calculated d values resulted from a least-squares treatment of the Guinier data.

occurrence of ferromagnetism at the Sr-rich end of the solid solution series as discussed in the magnetic section. Because the orthorhombic perovskite structure is somewhat complex, the relationship between the unit cell axes and individual MO_6 octahedra involved in superexchange interactions is obscured, especially for large departures from cubic symmetry. It is clear, however, that the RuO_6 octahedra in $SrRuO_3$ are more symmetrically

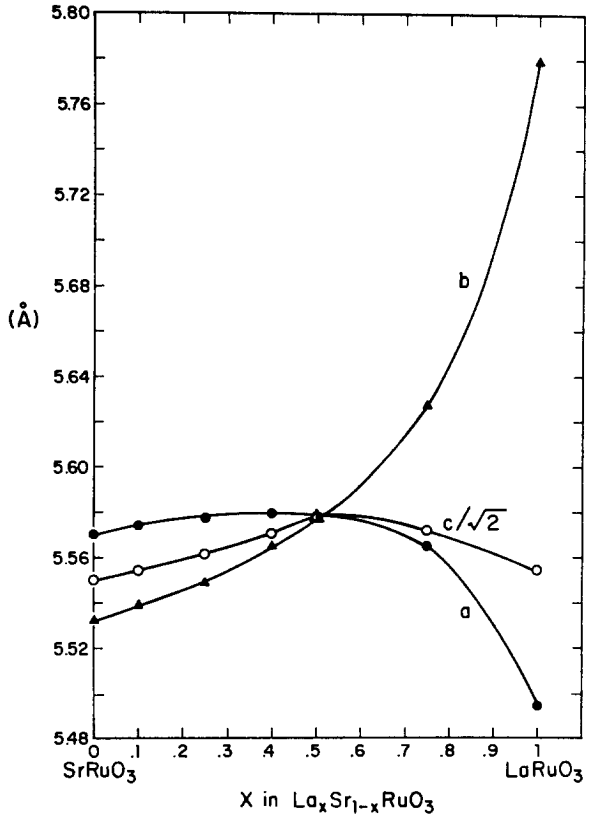

FIG. 1. The variation in lattice parameters vs. x in $La_xSr_{1-x}RuO_3$. $c/\sqrt{2}$ is plotted rather than c so as to better illustrate the distortion from cubic symmetry.

arranged, suggesting that overlap of Ru and O orbitals is maximized.

Wold et al. (*5*), who first reported $LaRuO_3$, noted that $NdRhO_3$ could also be prepared, but not $SmRhO_3$ or $YRhO_3$. It was assumed that the smaller size of Sm^{+3} and Y^{+3} could not satisfy the tolerance factor requirements for the stability of the perovskite phase. That is, for a given B^{+3} ion size, there is a minimum size requirement for the A ion, below which no perovskite can form. Since Ru^{+3} is larger than Rh^{+3}, it should be even more difficult to prepare any $MRuO_3$ where M is a rare earth ion smaller than La. This is in accord with experimental observations. $GdRuO_3$, $NdRuO_3$, and $PrRuO_3$ could not be prepared under the same conditions used for $LaRuO_3$. Instead, the pyrochlores, $A_2Ru_2O_7$, were the major phases. (However, single-phase $Nd_xSr_{1-x}RuO_3$ solid solutions could be prepared up to $x \sim 0.3$.) It therefore appears that compared to $MRhO_3$, the phase field defining the perovskite structure for $MRuO_3$ compounds is shifted further to the left in the lanthanide series so that only La^{+3}, the largest

ion, is included. In this connection, it may also be significant that no $La_2Ru_2O_7$ pyrochlore exists.

The almost universal adoption of the tetravalent state for Ru in oxides would seem to indicate a special stability. Therefore, Ru^{+3} should oxidize in air to Ru^{+4} at some reasonably low temperature. Surprisingly, $LaRuO_3$ can be heated in air to 700°C, suffering only a slight broadening of X-ray diffraction peaks after about 16 hr. At 900°C, the X-ray pattern becomes almost amorphous indicating destruction of the perovskite lattice.

B. Electrical

The electrical data plotted in Fig. 2 show a fairly low resistivity of approximately 5×10^{-3} ohm-cm for both $LaRuO_3$ and $La_{.5}Sr_{.5}RuO_3$. The positive temperature dependence is characteristic of metallic materials, but the low resistivity ratio and relatively high resistivity suggest that these oxides are poor "metals". It is fair to assume that the resistivity of single crystals would be considerably lower. Although the electrical results are qualitative, they do point to the same type of metallic-like behavior found for other Ru oxides like $SrRuO_3$ and RuO_2 (*2, 7*).

From qualitative band-model considerations of the type discussed by Goodenough (*8*), $LaRuO_3$ should be metallic with a 5/6-filled π^*-band formed from $(Ru)t_{2g} - (O)p\pi$ covalent interactions. A Seeback coefficient of $+42\ \mu V/°C$ was measured on a sintered piece of $LaRuO_3$ (hot junction = 60°C; cold junction = 27°C). The small positive voltage is consistent with hole conductivity in a nearly full band. The relatively high values for the resistivity may indicate that the conduction band is very narrow, leading to high masses and low mobilities; more likely, they result from the difficulties associated with resistivity measurements on polycrystalline samples.

If a model with a conduction band composed mainly of $t_{2g}(\pi^*)$ states is valid, the electrical properties of $LaRuO_3$ should be considerably different from $LaRuO_3$. For the latter, the 6-fold degenerate π^*-band should be completely filled (trivalent rhodium has a $4d^6$ configuration), leading to semiconducting properties, rather than metallic. Electrical conduction would then become an activated process, *via* transfer of electrons from $t_{2g}(\pi^*)$ to $e_g(\sigma^*)$ levels, which would presumably also exist as band states, σ-bonding being stronger than π-bonding. A crude 2-probe resistivity of about 1×10^4 ohm-cm. was measured on a pellet of $LaRhO_3$ at room temperature. This difference in resistivity of approximately seven orders of magnitude between $LaRuO_3$ and $LaRhO_3$ is consistent with a partially filled conduction band in the former and a filled band in the latter.

C. Magnetic

Magnetic susceptibility was measured as a function of temperature on five solid-solutions. The $1/\chi$ vs. T plots are shown in Fig. 3. To assure that the

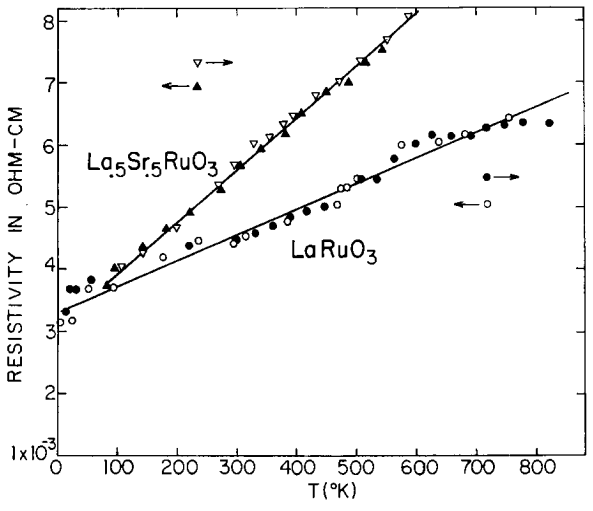

FIG. 2. The resistivity of $LaRuO_3$ and $La_{.5}Sr_{.5}RuO_3$ vs. temperature. Arrows indicate measurements taken on heating (→) or cooling (←).

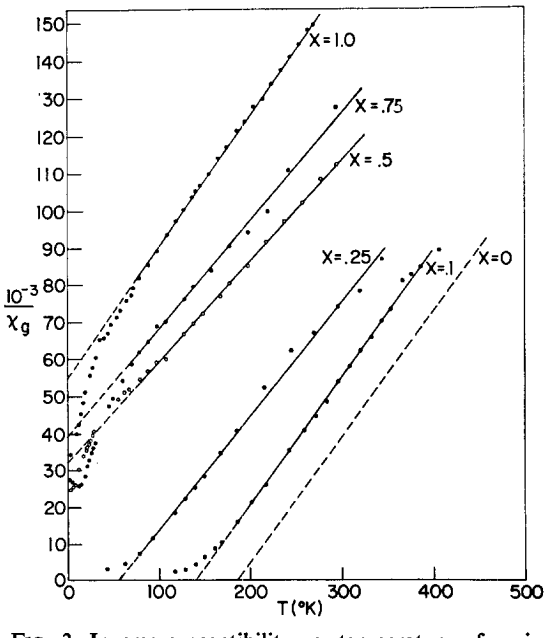

FIG. 3. Inverse susceptibility vs. temperature of various members of the $La_xSr_{1-x}RuO_3$ solid solution series. The data for $x = 0$ ($SrRuO_3$) were calculated from reference (2) and are included for comparison.

TABLE III[a]

Compound	C $\left(\frac{\text{emu °K}}{\text{mole Oe}}\right)$	μ_p (B.M.)	θ (°K)	μ_F (B.M.)	T_c (°K)	$\sigma_s(\frac{1}{H} \to 0, T \to 0)$ (emu/g)
$SrRuO_3$	—	2.65	+160	.85	160	
$La_{.1}Sr_{.9}RuO_3$	.709	2.39	+142	.75	133	17.4
$La_{.25}Sr_{.75}RuO_3$	.809	2.54	+59	.35	79	7.75
$La_{.5}Sr_{.5}RuO_3$	.946	2.75	−107	—	—	
$La_{.75}Sr_{.25}RuO_3$	.817	2.55	−127	—	—	
$LaRuO_3$	.841	2.59	−160	—	—	

[a] Magnetic parameters for $La_xSr_{1-x}RuO_3$. The $SrRuO_3$ data were taken from Ref. (2) and are included for comparison. The paramagnetic moment $\mu_p = [(3k/N\beta^2)\chi(T-\theta)]^{1/2}$ from susceptibility data in the Curie–Weiss region.

upper temperature portions of the curves correspond to the paramagnetic (Curie–Weiss) region, one sample was taken to high temperatures (Fig. 4). The calculated magnetic parameters are listed in Table III. No corrections were made for temperature independent contributions to the susceptibility because of the difficulty in accurately estimating this term. In addition to the negative contribution from core diamagnetism, there should be a positive Pauli contribution from conduction electrons. These are small, about the same order of magnitude, and tend to cancel one another.

All the compounds appear to show Curie–Weiss behavior at the higher end of the temperature region scanned. The straight line to 700°K for one sample supports this conclusion. The values for the paramagnetic moment are in the range 2.4–2.8 B.M., with no particular dependence on composition. Part of this fluctuation may be experimental error, although error propagation analysis indicates that the standard deviation in μ should be no greater than ~2% or ~±0.05 B.M. Another factor that is probably more important is the temperature range of the Curie–Weiss portion of the susceptibility data, which may be too small for the derivation of very accurate C and θ values. This is illustrated by the low and high temperature measurements on $La_{.75}Sr_{.25}RuO_3$, as shown in Figs. 3 and 4, respectively. Data in both temperature ranges were taken on the same sample preparation. From the high temperature run, $\mu = 2.56$ B.M. and $\theta = -127$°K (Table III). The corresponding low temperature data are 2.70 B.M. and −118°K. Given such scatter, no particular significance can be attached to the variation of μ with composition.

The formulas for the solid solutions can be written as $La_xSr_{1-x}Ru_x^{+3}Ru_{1-x}^{+4}O_3$. It can be safely assumed that both Ru^{+4} and Ru^{+3} are in the low-spin state

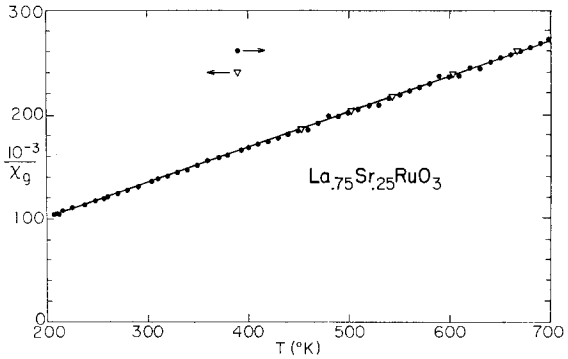

FIG. 4. Inverse susceptibility at high temperatures for $La_{.75}Sr_{.25}RuO_3$. Arrows indicate measurements taken on heating (→) or cooling (←).

because of strong covalency effects (large e_g–t_{2g} splitting) characteristic of 4*d*-ion interactions. An ESR study (*9*) of Ru^{+3} in a corundum (Al_2O_3) matrix confirms this even for the trivalent ion, where covalency should be weaker. The spin-only moments corresponding to the low-spin states of $Ru^{+3}(d^5)$ in $LaRuO_3$ and $Ru^{+4}(d^4)$ in $SrRuO_3$ are 1.73 and 2.83 B.M., respectively. Although $SrRuO_3$ appears to exhibit a paramagnetic moment near the spin-only value, the $LaRuO_3$ moment is considerably higher than expected. However, d^5 systems can show greatly enhanced paramagnetic moments (*10*, *11*) because of orbital contributions. While it may be tempting to contemplate the effect of a distorted octahedral environment on the Ru ion, a structure determination (*12*) of $GdFeO_3$ has shown that the distortion effected by the orthorhombic symmetry is mainly borne by Gd^{+3}, the Fe^{+3}–O octahedra remaining almost purely octahedral.

The most obvious trend in the magnetic properties of $La_xSr_{1-x}RuO_3$ is the appearance of antiferromagnetism with increasing x. The ferromagnetism

characteristic of $SrRuO_3$ disappears at approximately 35% La, where the Weiss constant θ becomes negative (Fig. 5).

The shapes of the $1/\chi$ vs. T curves for those samples that exhibit a negative θ are not completely typical of antiferromagnets. The lack of a pronounced minimum may mean weak parasitic ferromagnetism or trace ferromagnetic impurities. The only reasonable ferromagnetic impurity in the solid solution system would be $SrRuO_3$. Since the effect is present even for $LaRuO_3$, however, this seems unlikely to be the cause. Also, some of the curves are very similar to that of $CaRuO_3$ (*3*, *13*), which is thought to be an example of band antiferromagnetism with parasitic ferromagnetism below T_N. In addition, the fact that an orthorhombic distortion almost by definition prohibits exactly compensated antiferromagnetism suggests that parasitic ferromagnetism is a reasonable explanation for the magnetic behavior at low temperatures.

In an ABO_3 perovskite, both the A and the B ion compete in a covalent sense for the oxygen electrons. In $SrRuO_3$, Ru^{+4} is able to interact strongly because of its relatively high charge and small size. The two unpaired electrons in Ru t_{2g} levels are not localized on the Ru^{+4}, and can take part in ferromagnetic band interactions at low temperatures. Although paramagnetic behavior is found above T_c, the moment is below the spin-only value, consistent with some delocalization. When La^{+3} is substituted for Sr^{+2}, its smaller size and higher charge enable it to compete more strongly for oxygen electrons. At the same time, the Ru^{+3} resulting from the substitution is less strongly bonded than the Ru^{+4}, because of its larger size and smaller charge. These effects are additive, both leading to a decreasing Ru–O interaction, and presumably a narrower π^*-band. At $LaRuO_3$, the bandwidth has been sufficiently decreased so that antiferromagnetic behavior is observed, which appears to be more characteristic of narrow bands (*3*). The paramagnetic moment is considerably higher than the spin-only value; this may result from orbital contributions and has been observed, for example, in Ru complexes (*14*) where presumably the electrons are localized rather than collective. Evidence that the bandwidth has not decreased to zero is provided by the metallic-like electrical behavior.

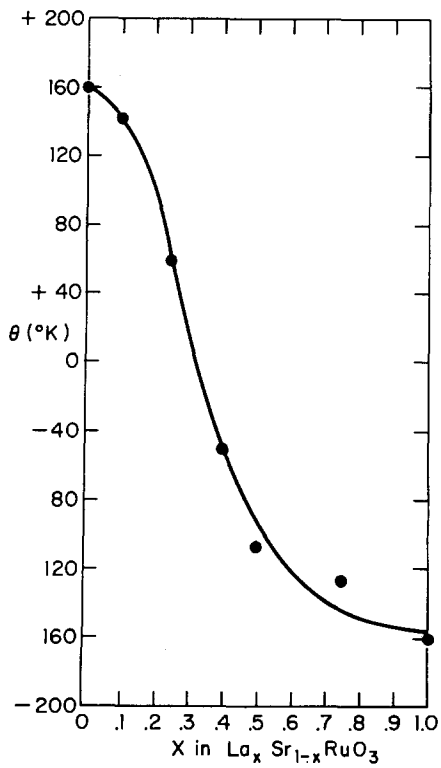

FIG. 5. Weiss constant θ vs. x for $La_xSr_{1-x}RuO_3$.

Similar reasoning was used (*3*) to explain the contrast between $CaRuO_3$ (antiferromagnetic, unit cell volume $V = 227$ Å^3) and $SrRuO_3$ (ferromagnetic, $V = 242$ Å^3). In that example, the more acidic Ca^{+2} decreased the strength of the Ru^{+4}–O interactions in $CaRuO_3$ to such an extent that antiferromagnetism resulted, *for the same number of d electrons per* Ru *ion*. Clearly the sign of the superexchange interaction between Ru ions is determined not so much by the *number* of d electrons in the π^* band as by other considerations such as Ru–O covalency and bandwidth of the π^* states.

Finally, the magnetic properties of $LaRhO_3$ should reflect the filled t_{2g} band previously discussed. This is essentially confirmed, with minor complications. A value of $\chi_g = 1.2 \times 10^{-7}$ emu/gm was found at 300°K. However, there was a small but definite temperature dependence and slight field dependence. The temperature dependence indicates a small amount of paramagnetic impurity ($C_m = 0.0082$, $\mu^2_{\text{eff}} = 0.066$; corresponds to 0.2 mole% of an $S = 5/2$ ion). The field dependence corresponds to a trace ferromagnetic component with a magnetization of $\sigma_g = 5.5 \times 10^{-4}$ emu.

Acknowledgments

Mrs. C. G. Frederick is thanked for the magnetic measurements on the ferromagnetic compounds; and so is Mr. J. L. Gillson for the electrical resistivity data. The comments and suggestions of Dr. D. B. Rogers are gratefully acknowledged,

as are several helpful discussions with Dr. A. W. Sleight concerning the crystallographic details of the perovskite structure.

References

1. J. B. GOODENOUGH, *J. Appl. Phys.* **37**, 1414 (1966).
2. A. CALLAGHAN, C. W. MOELLER, AND R. WARD, *Inorg. Chem.* **5**, 1572 (1966).
3. J. M. LONGO, P. M. RACCAH, AND J. B. GOODENOUGH, *J. Appl. Phys.* **39**, 1327 (1968).
4. J. J. RANDALL AND R. WARD, *J. Amer. Chem. Soc.* **81**, 2629 (1959).
5. A. WOLD, R. J. ARNOTT, AND W. J. CROFT, *Inorg. Chem.* **2**, 972 (1963).
6. R. D. SHANNON AND C. T. PREWITT, *Acta Crystallogr. B* **25**, 925 (1969).
7. J. M. FLETCHER, W. E. GARDNER, B. F. GREENFIELD, J. M. HOLDOWAY, AND M. H. RAND, *J. Chem. Soc. A* **1968**, 653.
8. J. B. GOODENOUGH, *Bull. Soc. Chim. Fr.* **1965**, 1200.
9. S. GESCHWIND AND J. P. REMEIKA, *J. Appl. Phys.* **33S**, 370 (1962).
10. M. KOTANI, *Progr. Theor. Phys.* Kyoto **14**, 1 (1960).
11. B. N. FIGGIS, J. LEWIS, R. S. HYHOLM, AND R. D. PEACOCK *Discuss. Faraday Soc.* **26**, 103 (1958).
12. P. COPPENS AND M. EIBSCHUTZ, *Acta Crystallogr.* **19**, 524 (1965).
13. J. B. GOODENOUGH, J. M. LONGO, AND J. A. KALAFAS, *Mater. Res. Bull.* **3**, 471 (1968).
14. B. N. FIGGIS, J. LEWIS, F. E. MABBS, AND G. A. WEBB, *J. Chem. Soc. A* **1966**, 422.